Full self-consistent Vlasov-Maxwell solution

Aurélien Cordonnier and Xavier Leoncini
Aix Marseille Univ, Université de Toulon, CNRS, CPT, Marseille, France

Guilhem Dif-Pradalier and Xavier Garbet
CEA, IRFM, F-13108 St. Paul-lez-Durance cedex, France

(Received 22 August 2022; accepted 30 November 2022; published 21 December 2022)

Full self-consistent stationary Vlasov-Maxwell solutions of magnetically confined plasmas are built for systems with cylindrical symmetries. The stationary solutions are thermodynamic equilibrium solutions. These are obtained by computing the equilibrium distribution function resulting from maximizing the entropy and closing the equations with source terms that are then computed by using the obtained distribution. This leads to a self-consistent problem corresponding to solving a set of two coupled second order nonlinear differential equations. Relevant plasma parameters are introduced and a bifurcation leading to an improvement of plasma confinement is shown. Conversely, in the improved confinement setting, we exhibit the emergence of a separatrix in the integrable motion of a charged particle .

DOI: 10.1103/PhysRevE.106.064209

I. INTRODUCTION

Within the scope of the search for better containment of Tokamak-based fusion plasma, understanding the emergence of transport barriers is a major issue. Indeed, they may give rise to the so-called H-mode which is at the heart of the current approach of magnetically confined fusion reactors. It now seems accepted that the internal transport barrier plays a major role in magnetized fusion plasma [1,2].

When considering magnetized fusion plasma, it is now commonly accepted that one of the best descriptions of the plasma is the kinetic one coupled to the Maxwell equations, and due to the low collisionality of the plasma the Maxwell-Vlasov system becomes the de facto first choice. The Vlasov equation is a common feature observed when considering systems with long range interactions, and beyond plasmas a large number of physical systems are in this category, like for instance gravitational forces and Coulomb interactions, vortices in two dimensional fluid mechanics [3–6], wave-particle systems relevant to plasma physics [7–9], and Free-Electron Lasers (FELs) [10,11]. In these settings, long range interacting Hamiltonian systems display some common dynamical features. Given some initial conditions, the systems exhibit a rapid relaxation towards a quasi-stationary state (QSS). These QSS have an extended lifetime, and one way to tackle them in statistical mechanics is to use the Lynden-Bell formalism [12,13]. In the realm of long range models the Hamiltonian mean field (HMF) model [14] has emerged as being a paradigmatic one, displaying most of the features observed in systems with long range interactions: nonadditivity [15], out of equilibrium phase transition [16,17], long lived quasi-stationary states, and slow relaxation towards equilibrium. More recently, the Hamiltonian microscopic dynamics has been investigated, displayed surprising regularity [18], and lead to the understanding of stationary states of the problem as a self-consistent infinite collection of uncoupled thus integrable pendula [19], and this could be extended to other models [20]. This regularity lead to the idea that long range systems organized themselves in terms of self-organized regularity [21], at least when it was possible, i.e., the underlying microscopic dynamics became integrable once an equilibrium was reached and the self-consistent fields were thus stationary. This was also the case for the true thermodynamic equilibrium. Given this feature, we will take a similar approach in the context of plasma physics and follow the recent results discussed in [22,23]. We construct complete thermodynamic equilibrium solutions of the classical Maxwell-Vlasov equations in a cylindrical geometry in the spirit of already discussed equilibria [24–28]. Indeed, in this geometry the motion of a charged particle in a two-component magnetic field can be made integrable, while it is not guaranteed in a toroidal configuration [29]. After applying the recipes we find stationary solutions of the Maxwell-Vlasov problem in this geometry, are obtained after solving a system of two coupled nonlinear ordinary differential equations. In this paper, these equations are computed and then solved, and regimes leading to a plasma confinement are discussed and investigated. The influence of plasma flows is thoroughly investigated and a bifurcation leading to an improved plasma confinement is presented; this is reminiscent, at least formally, to what one expects from the H-mode. Another important question that arises is whether or not the integrable individual microscopic dynamics resulting from the obtained self-consistent field can have a separatrix in their phase space. Indeed when only taking into account the self-consistency partially [22], it was shown that no separatrix could exist, while as will be shown, taking into account the full self-consistency can lead to the emergence of a separatrix. This feature is quite crucial, as it was shown in [29,30] that when moving to a toroidal configuration, the breaking of the separatrix was leading to

Hamiltonian chaos. Accompanying this chaos, large fluctuations of the magnetic moment are observed which therefore cannot be considered as an adiabatic invariant [31,32]. These observations might affect the foundations of gyrokinetics [33], and as such the results obtained through gyrokinetic simulations may not be considered as "first principles."

Finally, one last benefit of having exact solutions of the Vlasov-Maxwell system is that, besides their physical relevance for fusion plasmas, if proved to be stable, the solutions could be used as well as tests for numerical codes like, for instance, the one discussed in [34] as part of their verification process.

This paper is organized as follows. In the first part we briefly recall the recipes of the problem that were used in [22,23] and extend it by taking into account the poloidal current feedback. We also introduce the relevant physical plasma parameters that are at the core of our analysis. Then in Sec. II, we quickly derive the equations that allow us to study the different possible regimes, the full derivation, and computations of a two species plasma being derived in the Appendix. The solutions are studied in Sec. III, and a bifurcation between two regimes is exhibited and the individual microscopic dynamics is discussed. Finally, we conclude.

II. FULL SELF-CONSISTENT EQUILIBRIUM EQUATIONS

In this section we present the two nonlinear coupled ordinary differential equations that govern the self-consistent equilibrium solutions of the Maxwell-Vlasov problem in the considered cylindrical geometry. In order to do so, let us start by describing our considered setting.

A. Electromagnetic setting

We consider the problem of an infinite aspect ratio limit of an ideal Tokamak such that we can consider the torus as a cylinder and the usual cylindrical coordinates $(r,\ \theta,\ z)$ and associated unit vectors $(\mathbf{e}_r,\ \mathbf{e}_\theta,\ \mathbf{e}_z)$. In this setting, we consider a magnetic field with cylindrical symmetry $\mathbf{B}(\boldsymbol{r})$ in the following form

$$\mathbf{B} = \mathbf{B}_{\text{Plasma}} + \mathbf{B}_{\text{Ext}}, \tag{1}$$

where $\mathbf{B}_{\text{Ext}} = B_0\,\mathbf{e}_z$ is an external uniform magnetic field of intensity B_0 applied to the plasma, and $\mathbf{B}_{\text{Plasma}}$ is the magnetic field generated by the plasma. In order to comply with the symmetry we choose to consider magnetic fields that can be expressed as

$$\mathbf{B} = B_0[g(r)\,\mathbf{e}_\theta + (1 + k(r))\,\mathbf{e}_z], \tag{2}$$

where g and k are two functions that remain to be determined, and correspond to the plasma generated field, i.e., $\mathbf{B}_{\text{Plasma}} = B_0(g(r)\,\mathbf{e}_\theta + k(r)\,\mathbf{e}_z)$. From this we can get an expression of the vector potential

$$\mathbf{A} = A_\theta(r)\,\mathbf{e}_\theta + A_z(r)\,\mathbf{e}_z \tag{3}$$

in a Coulomb gauge which introduces two other related functions $K(r)$ and $G(r)$:

$$A_\theta(r) = \frac{B_0}{r}\int_0^r u(1 + k(u))\,du = \frac{B_0}{r}\left(\frac{r^2}{2} + K(r)\right), \tag{4}$$

and

$$A_z(r) = -B_0\int_0^r g(u)\,du = -B_0 G(r)\,. \tag{5}$$

So, the magnetic potential $\mathbf{A}(r)$ writes

$$\mathbf{A}(r) = B_0\left[\left(\frac{r}{2} + \frac{K(r)}{r}\right)\mathbf{e}_\theta - G(r)\,\mathbf{e}_z\right]. \tag{6}$$

Finally, we will assume that there is no electric field by, for instance, considering that there is some neutralizing background or that the charge density is zero using a two species approach (this is detailed in the Appendix).

B. Charged particle dynamics

We will consider the motion of a charged particle in the fields described previously. We shall assume that we have a classical non relativistic point particle with charge $Q = 1$ and mass $m = 1$. Using the canonical variables, the motion is Hamiltonian and the Hamiltonian of the system writes

$$H = \frac{(\mathbf{p} - \mathbf{A}(\mathbf{q}))^2}{2}, \tag{7}$$

where $\mathbf{p}$ and $\mathbf{q}$ form three pairs of canonically conjugate variables.

The associated equations of motions are

$$\begin{cases}\dot{\mathbf{q}} = & \mathbf{p} - \mathbf{A} \\ \dot{\mathbf{p}} = & \nabla\mathbf{A}.(\mathbf{p} - \mathbf{A})\end{cases}. \tag{8}$$

Given the specific form of the magnetic field and the associated symmetries (translation along z, and rotation around θ), the motion of charged particles is integrable and we can reduce the system to an effective one-dimensional Hamiltonian system

$$H = \frac{1}{2}\left[p_r^2 + \left(\frac{p_\theta}{r} - B_0\left(\frac{r}{2} + \frac{K(r)}{r}\right)\right)^2 + (p_z + B_0 G(r))^2\right] \tag{9}$$

$$= \frac{p_r^2}{2} + V_{\text{eff}}(r), \tag{10}$$

where p_θ and p_z are constants of the motion, see for instance [22].

C. Kinetic approach and equilibrium stationary distribution

In order to describe the plasma, we take a kinetic point of view and will consider a one particle distribution function at equilibrium in order to describe the physical state of the plasma. As mentioned we consider no electric field and neglect the collisions, so we can assume that the dynamics of the distribution function is governed by the Vlasov equation, and in our nonrelativistic setting it corresponds to the conservation of the particle distribution function along the trajectory of each particle, i.e.,

$$\frac{d}{dt}f(\mathbf{q}, \mathbf{p}, t) = 0, \tag{11}$$

where $\mathbf{q}$ and $\mathbf{p}$ satisfy (8). More information can be found in [35], for example. The particles are sources for the fields in

the Maxwell equations, and we have the source terms n for the spatial density function of charges, and $\mathbf{j}$ for the current vector, are given by

$$n(\mathbf{q},\mathrm{t}) = \int_{-\infty}^{+\infty} f(\mathbf{q},\mathbf{p},t)\, d^3p, \tag{12}$$

and

$$\mathbf{j}(\mathbf{q},t) = \int_{-\infty}^{+\infty} \mathbf{v} f(\mathbf{q},\mathbf{p},t)\, d^3p\,. \tag{13}$$

Since the motion of the particles is governed by the magnetic field, this implies a self-consistent problem [36]. In what follows we derive a possible candidate of the stationary distribution function by following the steps of the procedure described in [22,23]. Note that the full derivation of the equations is done in the Appendix, and for clarity we decided to go as straight as possible to the self-consistent equations to be solved.

When looking for a stationary solution of the nonself-consistent Vlasov equation (11), we can rewrite it with the usual Poisson bracket as

$$\{f, H\} = 0, \tag{14}$$

and so any function of H is a solution of the problem.

Furthermore, when building the distribution function coming from integrable microscopic motion we want to consider the fact that the total energy of the system H, the total momentum along z, and the total angular momentum along θ are conserved. Accordingly, the Poisson bracket with one of these conserved quantities is null. So, we can introduce respectively four Lagrange multipliers β, γ_z, γ_θ, and γ_0 in order to impose constraints corresponding to these conserved quantities, respectively, the energy, the momentum along z, the angular momentum, and the number of particles conservation (see [37,38] for quite similar approaches). And, in order to select a solution among the infinite possibilities, we settled for the one which maximizes the entropy

$$S[f] = -k_B \int_\Gamma f \ln(f)\, d\Omega, \tag{15}$$

where k_B is the Boltzmann constant and $d\Omega$ the infinitesimal volume of phase space Γ with the previously mentioned constraints. In order to fully characterize our problems we have to fix the number of particles N. However, since our geometry is the infinite cylinder, the actual relevant quantity is the particle density per unit length. Introducing an analogy with some kind of flat torus, we introduce a length scale, noted R, in the cylinder so that the particle density per unit length is noted $\lambda = N/2\pi R$. The solutions to this variational problem are given by a distribution of the form

$$f \propto e^{-\beta H - \gamma_z p_z - \gamma_\theta p_\theta}\,. \tag{16}$$

We can get the exact expression knowing the total number of particles N. Indeed, we choose to normalize f, such that

$$N = \int_\Gamma f\, d\Omega, \tag{17}$$

and so the proportionality constant in Eq. (16) is

$$f_0 = \frac{N}{4\pi^2 R\left(\frac{2\pi}{\beta}\right)^{3/2} \int_0^{+\infty} r e^{-ar^2 - bG(r) - cK(r) - \gamma_1}\, dr}, \tag{18}$$

with $\gamma_1 = -\frac{\gamma_z^2}{2\beta}$, $a = \frac{\gamma_\theta}{2}(B_0 - \frac{\gamma_\theta}{\beta})$, $b = -B_0\gamma_z$, and $c = B_0\gamma_\theta$. That leads to the final expression

$$f = \frac{N e^{-\beta H - \gamma_z p_z - \gamma_\theta p_\theta}}{4\pi^2 R\left(\frac{2\pi}{\beta}\right)^{3/2} \int_0^{+\infty} r e^{-ar^2 - bG(r) - cK(r) - \gamma_1}\, dr}\,. \tag{19}$$

It may be worth noting here that the β parameter corresponds to the thermodynamic temperature

$$\frac{1}{T} = \frac{\partial S}{\partial \mathcal{E}} = k_B\beta, \tag{20}$$

with the average energy $\mathcal{E}$ and it can be assumed positive. We also insist on the fact that γ_θ and γ_z are proportionalto the averages of $v_\theta = r\dot{\theta}$ and $v_z = \dot{z}$, respectively. In the literature [23], it has been noted that when a plasma rotation exists an internal transport barrier can exist. Then, it can be expected that in such states the statistical averages of v_θ and v_z are not null and so are γ_θ and $\gamma_{z,}$ respectively.

D. Sources of the plasma magnetic field

Always considering only one species of a charged particle with charge $q = 1$ and mass $m = 1$, we can compute the particle density and the current density in the plasma from the form of the resulting distribution function (19) and the Hamiltonian (9), and extract an explicit form of the source terms which depends on the functions G and K. For instance, the spatial density n behaves like

$$n(\mathbf{q}) \propto e^{-ar^2 - bG(r) - cK(r)}\,. \tag{21}$$

We can also compute the proportionality term in Eq. (21) and express the radial density ρ given by

$$\rho(r) = \frac{\int n(\mathbf{q})\, r\, d\theta\, dz}{\int r\, d\theta\, dz} = \frac{1}{4\pi rR}\int n(\mathbf{q})\, r\, d\theta\, dz, \tag{22}$$

as

$$\rho(r) = \frac{1}{\mathscr{V}} e^{-ar^2 - bG(r) - cK(r)}, \tag{23}$$

with

$$\mathscr{V} = \frac{4\pi^2 R \int_0^{+\infty} r e^{-ar^2 - bG(r) - cK(r)} dr}{N}\,. \tag{24}$$

We notice that as discussed in [23], Eq. (23) shows that the equilibrium profile is not flat as soon as γ_θ is not zero and it depends on the poloidal magnetic field configuration when $\gamma_z \neq 0$. In other words as soon as the plasma has nonvanishing angular momentum the profiles are not flat. Moreover, since we consider an equilibrium configuration, we also obtain a

nonflat temperature profile but we have to consider the local radial kinetic temperature profile, rather than the thermodynamic one (20) discussed previously. For instance we can compute the average kinetic energy at a constant radius

$$\varepsilon(\mathbf{q}) = \int H f \, d^3p, \tag{25}$$

that leads to

$$\varepsilon(\mathbf{q}) = \frac{\partial n(\mathbf{q})}{\partial \beta}, \tag{26}$$

which implies that the radial kinetic energy profile is, akin to an ideal gas, related to the radial density and therefore has the same shape.

In the same spirit we now compute the source terms of the plasma magnetic field and move to the current density $\mathbf{j}$. We start directly from (13) and the speeds

$$v_z = p_z + B_0 G(r), \tag{27}$$

and

$$v_\theta = \frac{p_\theta}{r} - B_0\left(\frac{r}{2} + \frac{1}{r}K(r)\right). \tag{28}$$

So, if we break down $\mathbf{j}$ by component, the density current along the θ coordinate is given by

$$j_\theta(\mathbf{q}) = \int_{-\infty}^{+\infty} v_\theta f \, dp_r \, d\frac{p_\theta}{r} dp_z, \tag{29}$$

and ends up as

$$j_\theta(\mathbf{q}) = -\frac{1}{\mathscr{V}}\frac{\gamma_\theta}{\beta} r e^{-ar^2 - bG(r) - cK(r)}. \tag{30}$$

For the density current along the z coordinate, we do the same

$$j_z(\mathbf{q}) = \int_{-\infty}^{+\infty} v_z f \, dp_r \, d\frac{p_\theta}{r} dp_z, \tag{31}$$

and we obtain

$$j_z(\mathbf{q}) = -\frac{1}{\mathscr{V}}\frac{\gamma_z}{\beta} e^{-ar^2 - bG(r) - cK(r)}. \tag{32}$$

So we finally find

$$\mathbf{j}(\mathrm{r}) = -\frac{1}{\mathscr{V}}\left(\frac{\gamma_\theta}{\beta} r\, \mathbf{e}_\theta + \frac{\gamma_z}{\beta}\, \mathbf{e}_z\right) e^{ar^2 - bG(r) - cK(r)}, \tag{33}$$

or when rewritten as a function of radial density:

$$\mathbf{j}(\mathrm{r}) = -\left(\frac{\gamma_\theta}{\beta} r\, \mathbf{e}_\theta + \frac{\gamma_z}{\beta}\, \mathbf{e}_z\right)\rho(r). \tag{34}$$

Now that the source terms have been computed we may move to the self-consistent solutions. However, we can already notice that the solutions will obey an interesting condition that is independent of the thermodynamic temperature:

$$\frac{j_\theta(\mathrm{r})}{r j_z(\mathrm{r})} = \frac{\gamma_\theta}{\gamma_z}. \tag{35}$$

E. General Self-Consistent Equation

1. Self-consistent system and reduction

We have computed the currents which depend on the functions K and G that are defining the vector potential (6) in Coulomb gauge ($\nabla \cdot \mathbf{A} = 0$) which itself is related to the current through Ampère's law and ends up to be a Poisson equation

$$\Delta \mathbf{A} = -\mu_0 \mathbf{j}, \tag{36}$$

and so, using the previously computed source terms we obtain a set of self-consistent equation

$$\begin{cases} \frac{1}{r}\frac{\partial}{\partial r}\left(\frac{1}{r}\frac{\partial}{\partial r}K(r)\right) = \kappa_\theta e^{-ar^2 - bG(r) - cK(r)} \\ \frac{1}{r}\frac{\partial}{\partial r}\left(r\frac{\partial}{\partial r}G(r)\right) = -\kappa_z e^{-ar^2 - bG(r) - cK(r)}, \end{cases} \tag{37}$$

with

$$\kappa_{\theta/z} = \frac{\mu_0}{B_0 \beta \mathscr{V}} \gamma_{\theta/z}. \tag{38}$$

A full derivation of these equations when considering a two species neutral plasma is performed in the Appendix, and we end up with the same form as expressions (37).

Let us now study the system more (37). First, in order to simplify and given the relation (35), we rescale the length using a scaling of the type $\widetilde{r} \to \frac{\gamma_\theta}{\gamma_z} r$. Furthermore, if we also do the transformations $\widetilde{G}(r) \to bG(r)$ and $\widetilde{K}(r) \to ar^2 + cK(r)$, and finally we set $\widetilde{j}_z(\widetilde{r}) = \alpha e^{-\widetilde{G}(\widetilde{r}) - \widetilde{K}(\widetilde{r})}$ where $\alpha = \frac{(b\kappa_z)^2}{c\kappa_\theta}$ for the current density, we end up with

$$\begin{cases} \frac{1}{\widetilde{r}}\frac{\partial}{\partial \widetilde{r}}\left(\frac{1}{\widetilde{r}}\frac{\partial}{\partial \widetilde{r}}\widetilde{K}(\widetilde{r})\right) = \widetilde{j}_z(\widetilde{r}) \\ \frac{1}{\widetilde{r}}\frac{\partial}{\partial \widetilde{r}}\left(\widetilde{r}\frac{\partial}{\partial \widetilde{r}}\widetilde{G}(\widetilde{r})\right) = \widetilde{j}_z(\widetilde{r}) \end{cases}. \tag{39}$$

For convenience we now omit the $\widetilde{\ }$, and forget the z in j_z. Also, since we only have functions depending on r, partial derivatives are simple ones. Working with Eq. (39) we have

$$\frac{1}{r}\frac{d}{dr}\left(\frac{1}{r}\frac{dK(r)}{dr}\right) = \frac{1}{r}\frac{d}{dr}\left(r\frac{dG(r)}{dr}\right), \tag{40}$$

and obtain

$$\frac{dK(r)}{dr} = r^2\frac{dG(r)}{dr} + \alpha_0 r, \tag{41}$$

with the integration constant α_0 that will need to be determined. Then from the logarithmic derivative of $j(r)$ we obtain

$$\frac{1}{j(r)}\frac{dj}{dr} = -\frac{dG(r)}{dr} - \frac{dK(r)}{dr}. \tag{42}$$

And by combining these equations and differentiating (42) we end up with

$$\frac{d^2 j}{dr^2} = -\left(\frac{2\alpha_0}{1+r^2} + (1+r^2)j\right)j + \left(\frac{1}{j}\frac{dj}{dr} - \frac{1-r^2}{r(1+r^2)}\right)\frac{dj}{dr}. \tag{43}$$

So we end up with one second order nonlinear ordinary differential equation, which once solved gives us the whole properties of the self-consistent Vlasov-Maxwell stationary state. Before solving it let us first discuss the conditions that

need to be met for typical physical expected conditions, we insist that in contrast to the analytical work performed [22], here the full self-consistent field is taken into account and possible moderation effects on the external magnetic field are taken into account, leading to a set of differential equations (37) instead of just one.

2. Constraints and parameters

Let's take a closer look at the parameters necessary for the integration of (43) in order to construct our Vlasov-Maxwell stationary solutions. Given the symmetry of the problem, it is natural to expect that $\frac{dj}{dr}(0) = 0$, so only two parameters α_0 and $j(0)$ are needed to obtain the solution of (39). Then after fixing the plasma constants we will have access to the full Vlasov-Maxwell solution. The problem lies in connecting these two parameters with the global equilibrium parameters of the plasma which are β, γ_z, and γ_θ, and also connect these to the external parameters, B_0 and the lineic average plasma density $\lambda = N/2\pi R$. Note that we will assume that the unit length, i.e., the typical scale on which particles are confined, or a typical radius of the cylinder to be equal to 1, so $1/R$ has no dimension and can be more considered like, for instance, an aspect ratio if we imagine the cylinder as the limit of a torus. We shall now attempt to compute the two parameters from the global parameters, and start our analysis with α_0.

For this purpose let us recall Eq. (41) and compute the constant in $r = 0$. Tracing back we obtain

$$\alpha_0 = \left(\frac{\gamma_z}{\gamma_\theta}\right)^2 \left[2a + c\left(\frac{1}{r}\frac{\partial K}{\partial r}\right)\bigg|_{r=0}\right] - b\left(r\frac{\partial G}{\partial r}\right)\bigg|_{r=0}. \quad (44)$$

On the one hand, $(r\frac{\partial G}{\partial r})|_{r=0} = 0$ [from (5) we note that $\frac{\partial G(r)}{\partial r} = g(r)$ and $g(r)$ is bounded]. On the other hand, from (4) we note that $(\frac{1}{r}\frac{\partial K}{\partial r})|_{r=0} = k(0)$. Given the cylindrical geometry, along z and for $r = 0$, the magnetic field $B_z(0)$ corresponds to the sum of the external B_0 field and the sum of infinitesimal uniform fields generated by infinitesimal solenoids of thickness dr. These correspond in fact to the field generated by the current per unit length $\frac{I_\theta}{2\pi R} = \int_0^{+\infty} j_\theta(r)dr$. So we end up with

$$\begin{aligned} k(0) &= \frac{\mu_0}{B_0}\int_0^{+\infty} j_\theta(r)dr \\ &= -\frac{\mu_0}{B_0}\frac{N}{4\pi^2 R}\frac{\gamma_\theta}{\beta}, \end{aligned} \quad (45)$$

and thus

$$\alpha_0 = \frac{\gamma_z^2}{\gamma_\theta}\left(B_0 - \frac{\gamma_\theta}{\beta}\right) - \mu_0\frac{\gamma_\theta^2 N}{4\pi^2 R\beta}. \quad (46)$$

Regarding $j(0)$, since the vector potential is defined up to some constants, we end up with

$$j(0) = \alpha = \frac{(b\kappa_z)^2}{c\kappa_\theta} = \frac{\gamma_z^4}{\gamma_\theta^2}\frac{\mu_0}{\beta\mathscr{V}}. \quad (47)$$

Unfortunately $\mathscr{V}$ depends on the integral of the function $rj(r)/j(0)$, $j(r)$ depends on $j(0)$, and the differential equation (43) is nonlinear, so we have some implicit problem. Fortunately we also have some constant parameters in $\mathscr{V}$, that we may adjust. So the strategy in what follows will be to fix a value of α_0 and a value of $j(0)$, so we can obtain the function $j(r)$, from which the equilibrium will be defined.

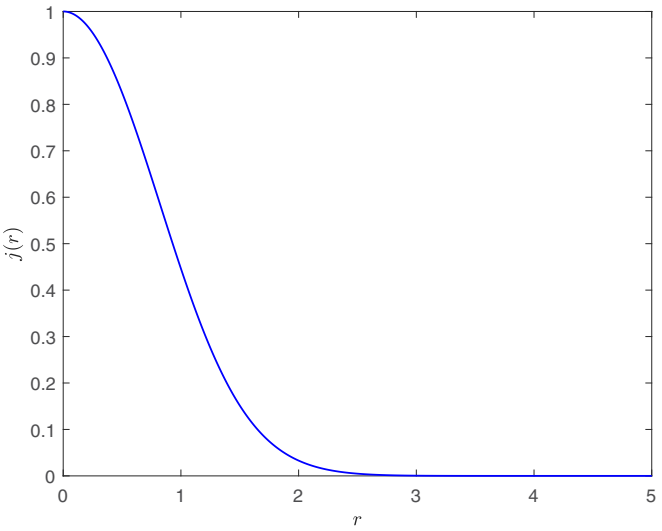

FIG. 1. Typic al density profile here obtained with $j(0) = \alpha_0 = 1$.

III. SOLUTIONS

A. Standard equilibrium profiles

From the form of the solutions (43) and having the constants, (46) and (47), more or less defined from plasma parameters, we can now compute and sketch some density current profiles. Note that we also consequently have access to the density profile since $\rho(r) \propto n(\mathbf{q}) \propto j(r)$. In order to plot these profiles, we have to choose values for the parameters set $(j(0), \alpha_0)$. The solutions from the differential equation (43) are computed using octave (lsode) [39]. As we expected from [22], we also get nonflat "Gaussian" type profiles for a given cho ice of parameters (see figure 1). The quantity $j(0)$, as we can expect, is linked to the height of the $j(r)$ curve, conversely α_0 appears to influence the shape of the profile.

B. Bifurcation towards enhanced confinement profiles

Regarding the behavior of the profile, for a fixed value of $j(0)$, a bifurcation with the emergence of a positive curvature and an enhanced density profile near $r = 0$ can be identified. To do so, we make some Taylor expansions near $r = 0$ and use the self-consistent Eq. (43). We find that the threshold $\frac{\partial^2 j}{\partial r^2}|_{r=0} = 0$ is obtained when

$$\frac{j(0)}{-2\alpha_0} = 1, \quad (48)$$

from which we obtain solutions where the profiles exhibit a maximum in $r = 0$ and others with "eccentric" profiles, i.e., a maximum of the density function for a given $r_0 > 0$. In order to study the different shape of solutions we choose to fix

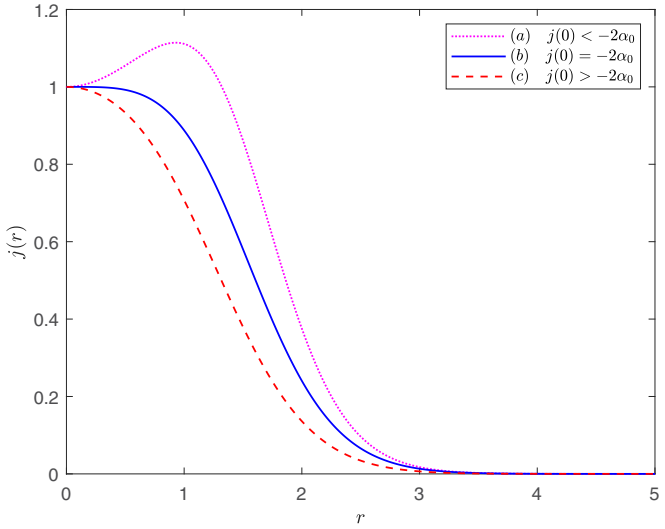

FIG. 2. Density profiles with $j(0) = \alpha = 1$. (a) with $\alpha_0 = -1$, (b) with $\alpha_0 = -1/2$, (c) with $\alpha_0 = 0$. The critical bifurcation value is $\alpha_0 = -1/2$, we see an enhanced density profile emerging for $\alpha_0 < -1/2$.

$j(0) = 1$ and we tune the parameter α_0, results are displayed in figure 2.

We can notice also the role of the poloidal current density $j_\theta(r)$ depicted in figure 3, tends to be stronger and more peaked, i.e., localized, once the bifurcation is crossed.

C. Link to hyperbolic points

Some evidence that steeper density profiles could be linked to the presence of hyperbolic points in particle trajectories have been made in [23]. In order to check if this is still the case with a self-consistent solution let us consider the effective potential defined in Eq. (10) and rewrite it with the scaled

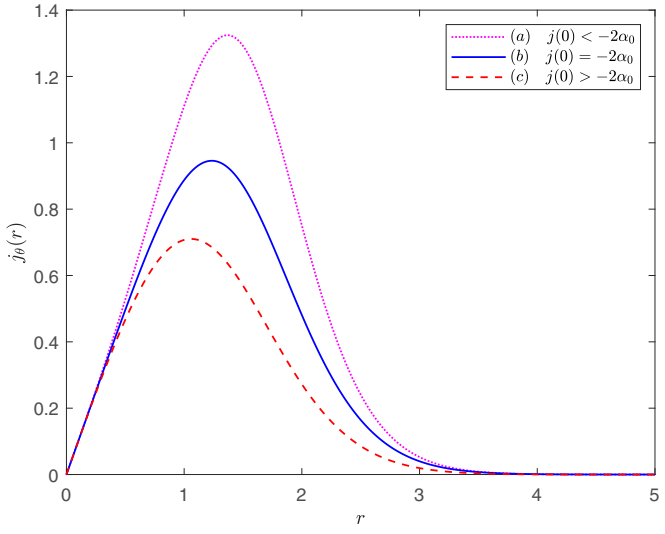

FIG. 3. $j_\theta(r)$ profiles with $j(0) = \alpha = 1$. (a) with $\alpha_0 = -1$, (b) with $\alpha_0 = -3/2$, (c) with $\alpha_0 = 0$. The critical bifurcation value is $\alpha_0 = -1/2$, we see that the current profile gets more peaked when $\alpha_0 < -1/2$.

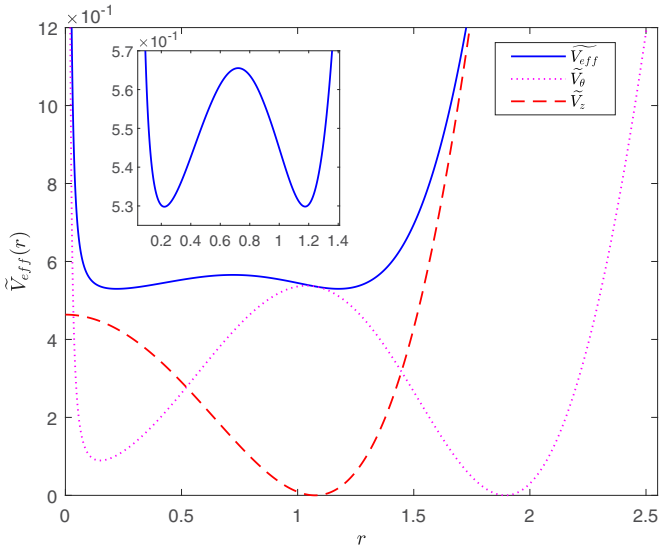

FIG. 4. Effective potential $\widetilde{V}_{\text{eff}} = \beta V_{\text{eff}}$ as a function of r rescaled by r_γ, with $j(0) = 1$, $\alpha_0 = -1$, $p_\theta = 0.01$, and $p_z \approx 0.30$. Both contributions of the term involving G (dubbed $\tilde{V}_z$) and the one involving K (dubbed $\tilde{V}_\theta$) are represented. Both are needed to explain the shape of the double well potential highlighted in the insert.

variables, we obtain

$$\beta V_{\text{eff}}(r) = \frac{\beta}{2\gamma_z^2}\left[\left(\frac{p_\theta}{r} - \left(\frac{\gamma_z^2}{\beta}\frac{r}{2} + \frac{K(r)}{r}\right)\right)^2 + (p_z - G(r))^2\right]. \tag{49}$$

To look for hyperbolic points, we need to check the shape of this potential, which obviously does not depend directly on γ_z, but we have to choose a value for the particle density λ to determine an effective potential. In order to be somewhat realistic, we settled for an ITER like value of the parameter and fixed $\frac{\gamma_z^2}{\beta} = \beta\langle v_z\rangle^2 \sim 0.1$, with the orders of magnitude and notations developed in section III D. We recall that here the functions G and K are actually $\tilde{G}$ and $\tilde{K}$ which are solutions of the self-consistent equations (39), which thus depend on the plasma parameters. Now, exploring the shape of the potential for different values of p_θ and p_z, we find that there are effective potentials that give rise to unstable hyperbolic fixed points (see figure 4), we find these potentials once we have crossed the bifurcation threshold.

It is important also to point out the influence of diamagnetic effects due to the poloidal current. Indeed, when neglecting these effects it was not possible to obtain effective potentials with hyperbolic points (see [22]). In fact, in figure 4 we can see the individual contribution of both terms in the effective potential, namely the one involving G and the one involving K, and one clearly sees that both are needed to create the hyperbolic points in between the two two stable elliptic points. Moreover the presence of such effective potentials above the bifurcation threshold that creates an enhanced density profile is also consistent with the results depicted in [23]. This phenomenon could indeed be important as any perturbation will break the separatrix and lead to Hamiltonian chaos. This could occur, for instance, in toroidal magnetic fields configurations

with large aspect ratios which can lead to chaos and destroy the magnetic moment, impacting as such the reliability of gyrokinetic simulations.

D. Back to plasma parameters

Now that we have briefly analyzed the solutions that we get, we want to summarize what are the plasma parameters corresponding to these solutions and discuss the m. We list them in three categories:
(a) External constraints: R, $B_{0,}$
(b) Microscopic physics: m^-, m^+, q^-, q^+
(c) Plasma parameters: N, β, γ_θ, $\gamma_{z.}$
We shall below consider only the one species solution discussed previously. We recall that the characteristic length scale of the systems is given by

$$r_\gamma = \frac{\gamma_z}{\gamma_\theta}\,. \tag{50}$$

We then have α_0 given by Eq. (46) and $j(0)$ by Eq. (47).

We can then, for instance, compute the poloidal and toroidal current by computing the flux of $\boldsymbol{j}$, that leads to the currents

$$I_\theta = -\frac{qN}{2\pi}\frac{\gamma_\theta}{\beta}, \tag{51}$$

$$I_z = -\frac{qN}{2\pi R}\frac{\gamma_z}{\beta}, \tag{52}$$

or the typical speed of the plasma along both directions

$$\frac{\langle \boldsymbol{v}\rangle}{N} = -\begin{pmatrix} 0 \\ \frac{\gamma_\theta}{\beta}\frac{\langle r\rangle}{N} \\ \frac{\gamma_z}{\beta} \end{pmatrix}. \tag{53}$$

We may as well compute the energy density

$$\frac{\langle H\rangle}{N} = \left[\frac{3}{2\beta} + \frac{m\gamma_\theta^2}{2\beta^2}\frac{\langle r^2\rangle}{N} + \frac{m\gamma_z^2}{2\beta^2}\right] \tag{54}$$

that corresponds to the average kinetic energy of the particles. We see here that due to the plasma flow we do not have the usual direct link between β, and the kinetic energy per particle and additional terms appear.

In order to see if these stationary solutions could be relevant in the context of magnetized fusion, we also compute some order of magnitudes, considering $T \sim 10$ keV, $B_0 \sim 1$ T, $N \sim 10^{20}$ m^{-3}, $m \sim 10^{-27}$ kg, and $Q = e$. Let us consider a distribution with $a \sim 10$, $b \sim 10$, and $c \sim 10$, like what was done in [23]; we also want our typical scale r_γ to be of the order of the small radius of a tokamak, so about 1 m, and some aspect ratio of order 1/3, this means $\gamma_z \sim \gamma_\theta$. With these values, we end up with $\langle v_z\rangle \sim \langle v_\theta\rangle \sim c/1000$, c being the speed of light. Also, $\gamma_z \sim \gamma_\theta \sim \beta\langle v\rangle \sim 5\,10^{-10}$ USI (corresponding to the international units, note γ_z and γ_θ do not have the same dimensions, but $r \sim 1$). We can also estimate the current $I_z \sim 5\,10^5$ A. These estimations are in line with typical scales of parameters in magnetized fusion machines. We may thus anticipate that these stationary solutions could be relevant in the fusion context, and especially the exhibited bifurcation.

IV. CONCLUSION AND PERSPECTIVES

In this paper we have computed a family of stationary solutions to the Vlasov-Maxwell equations, in a cylindrical geometry. These solutions correspond to a thermodynamic equilibrium and display a nonuniform density profile at equilibrium, also with a nonuniform kinetic temperature profile as soon as the plasma displays nonvanishing angular momentum, i.e., collective motion in the poloidal or the toroidal. This simple feature is already somewhat counter intuitive as the commonly accepted paradigm in tokamak physics is that these nonuniform profiles are the result of out of equilibrium features, with energy injection at the center and dissipation at the walls, so these solutions with global plasma momentum are offering a possibly different perspective on the confinement. As shown, the solutions are obtained from applying an entropy maximization principle from which a probability density function is obtained, and then a self-consistent equation has to be solved on the vector potential using the Maxwell-Ampère equation that looks like a Poisson equation and ends up in solving two coupled nonlinear second order ordinary differential equations. The solutions are described using three intensive variables β, γ_z, and γ_θ corresponding to the Lagrange multipliers related respectively to energy, momentum, and angular momentum conservations. From these parameters a typical scale on which plasma confinement is observed r_γ emerges and depends only on the ratio of γ_z and γ_θ, and is as such independent of the global temperature. Moreover, diamagnetic effects play an important role and a bifurcation between solutions showing an enhanced confinement profile from a more regular one is displayed and the threshold computed. Finally, when the bifurcation is crossed and confinement is enhanced, there are regions in phase space where individual particles are subject to a double well potential exhibiting a separatrix. The presence of this separatrix in these enhanced confinement profile is consistent to what was previously anticipated in a non self-consistent setting [23] and are also roots for Hamiltonian chaos under any perturbations that can also break the magnetic moment conservation [29] and create some possible problems regarding the validity of gyrokinetic simulations.

Even though computed through a maximizing principle, the stability of these solutions under, for instance, a small perturbation like moving the system to a torus with a large aspect ratio is not at all given. A perspective of this work would then be to assess the stability of these solutions, to also check what happens near the chaotic separatrices and the breaking of the magnetic moment when moving to a real toroidal geometry where poloidal symmetry is lost or when adding the possibility to develop electric fields.

ACKNOWLEDGMENTS

This work has been carried out within the framework of the EUROfusion Consortium, funded by the European Union via the Euratom Research and Training Programme (Grant Agreement No. 101052200 — EUROfusion). Views and opinions expressed are however those of the author(s) only and do not necessarily reflect those of the European Union or the

European Commission. Neither the European Union nor the European Commission can be held responsible for them.

APPENDIX: GENERALIZATION TO A TWO SPECIES SYSTEM WITH CHARGES q^+ AND q^-, AND MASS m^+ AND m^-

Below, we derive the full self-consistent system that gives rise to a stationary solution of the Vlasov-Maxwell system. We follow the same path as the one used for only one species. We use the notation with a + or a - at the upper corner to simplify the notations corresponding to each species, for example, the test particle Hamiltonians write

$$H^{\pm} = \frac{(\mathbf{p}^{\pm} - q^{\pm}\mathbf{A})^2}{2m^{\pm}}, \tag{A1}$$

and then lead to the distributions functions

$$f^{\pm} = f_0^{\pm} e^{-\beta H^{\pm} - \gamma_z^{\pm} p_z^{\pm} - \gamma_\theta^{\pm} p_\theta^{\pm} - \gamma_1^{\pm}}, \tag{A2}$$

after the Lagrange multipliers introduction and maximization of the entropy. Note that by doing so, we assume that the entropy is additive so the global maximum may be the sum of two maxima taken for each species individually, which somehow neglect the couplings through the current, for instance, so this may not be a thermodynamic equilibrium in the end, but anyhow, this leads to a stationary solution of the Vlasov-Maxwell system. We assume that each distribution is a stationary solution of the Vlasov so that

$$\{f^{\pm}, H^{\pm}\} = 0\,. \tag{A3}$$

If we take $a^{\pm} = \frac{\gamma_\theta^{\pm}}{2}(q^{\pm}B_0 - \frac{m^{\pm}\gamma_\theta^{\pm}}{\beta^{\pm}})$, $b^{\pm} = -q^{\pm}B_0\gamma_z^{\pm}$, $c^{\pm} = q^{\pm}B_0\gamma_\theta^{\pm}$ and $\gamma_1^{\pm} = -\frac{m^{\pm}(\gamma_z^{\pm})^2}{2\beta^{\pm}}$, the normalization of each distribution function can be derived through

$$\begin{aligned} N^{\pm} &= \int f^{\pm}\, d^3p^{\pm} d^3q^{\pm} \\ &= f_0^{\pm} 4\pi^2 R \left(\frac{2\pi m^{\pm}}{\beta^{\pm}}\right)^{3/2} \int_0^{+\infty} r e^{-a^{\pm}r^2 - b^{\pm}G(r) - c^{\pm}K(r) - \gamma_1^{\pm}} dr, \end{aligned} \tag{A4}$$

for $N^{\pm}$ the numbers of particles. So the normalization of f is

$$f_0^{\pm} = \frac{N^{\pm}}{4\pi^2 R \left(\frac{2\pi m^{\pm}}{\beta^{\pm}}\right)^{3/2} \int_0^{+\infty} r e^{-a^{\pm}r^2 - b^{\pm}G(r) - c^{\pm}K(r) - \gamma_1^{\pm}} dr}\,. \tag{A5}$$

We can then compute the spatial densities for each species

$$\begin{aligned} n^{\pm}(\mathbf{q}) &= \int f^{\pm}\, d^3p^{\pm} \\ &= \frac{N^{\pm} e^{-a^{\pm}r^2 - b^{\pm}G(r) - c^{\pm}K(r)}}{4\pi^2 R \int_0^{+\infty} r e^{-a^{\pm}r^2 - b^{\pm}G(r) - c^{\pm}K(r)} dr}, \end{aligned} \tag{A6}$$

and the charge radial density

$$\begin{aligned} \rho^{\pm}(r) &= q^{\pm} \frac{\int n^{\pm}(\mathbf{q}) r\, d\theta\, dz}{\int r\, d\theta\, dz} \\ &= \frac{q^{\pm}}{\mathscr{V}^{\pm}} e^{-a^{\pm}r^2 - b^{\pm}G(r) - c^{\pm}K(r)}, \end{aligned} \tag{A7}$$

with $\mathscr{V}^{\pm} = \frac{4\pi^2 R \int_0^{+\infty} r e^{-a^{\pm}r^2 - b^{\pm}G(r) - c^{\pm}K(r)} dr}{N^{\pm}}$. In order to move to self consistency, we also compute, by component, the currents densities induced. Since

$$v_z^{\pm} = \frac{1}{m^{\pm}}(p_z^{\pm} - q^{\pm}B_0 G(r)) \tag{A8}$$

and

$$v_\theta^{\pm} = \frac{1}{m^{\pm}}\left(\frac{p_\theta^{\pm}}{r} - q^{\pm}B_0\left(\frac{r}{2} + \frac{1}{r}K(r)\right)\right), \tag{A9}$$

after integration we obtain $j_\theta^{\pm}(\mathbf{q})$ and $j_z^{\pm}(\mathbf{q})$, so the full current densities are given by

$$\mathbf{j}^{\pm}(r) = -\frac{1}{\beta^{\pm}}(\gamma_\theta^{\pm} r\, \mathbf{e}_\theta + \gamma_z^{\pm}\, \mathbf{e}_z)\rho^{\pm}(r)\,. \tag{A10}$$

Furthermore, we point out the relations

$$\frac{j_\theta^{\pm}(\mathbf{q})}{r j_z^{\pm}(\mathbf{q})} = \frac{\gamma_\theta^{\pm}}{\gamma_z^{\pm}}\,. \tag{A11}$$

We now move to the full self-consistent equation. We remain in Coulomb gauge ($\nabla \cdot \mathbf{A} = 0$), so we have

$$\Delta \mathbf{A} = -\mu_0(\mathbf{j}^+ + \mathbf{j}^-), \tag{A12}$$

and we end up with the self-consistent equation

$$\begin{cases} \frac{1}{r}\frac{\partial}{\partial r}\left(\frac{1}{r}\frac{\partial}{\partial r}K(r)\right) = \frac{\mu_0}{B_0}\left[\frac{\gamma_\theta^+}{\beta^+}\rho^+(r) + \frac{\gamma_\theta^-}{\beta^-}\rho^-(r)\right] \\ \frac{1}{r}\frac{\partial}{\partial r}\left(r\frac{\partial}{\partial r}G(r)\right) = -\frac{\mu_0}{B_0}\left[\frac{\gamma_z^+}{\beta^+}\rho^+(r) + \frac{\gamma_z^-}{\beta^-}\rho^-(r)\right] \end{cases}. \tag{A13}$$

We recall that we are assuming no electric field, so we have to impose electroneutrality

$$\rho^+(r) + \rho^-(r) = 0, \tag{A14}$$

which implies

$$\begin{cases} \frac{1}{r}\frac{\partial}{\partial r}\left(\frac{1}{r}\frac{\partial}{\partial r}K(r)\right) = \frac{\mu_0}{B_0}\left[\frac{\gamma_\theta^+}{\beta^+} - \frac{\gamma_\theta^-}{\beta^-}\right]\rho^+(r) \\ \frac{1}{r}\frac{\partial}{\partial r}\left(r\frac{\partial}{\partial r}G(r)\right) = -\frac{\mu_0}{B_0}\left[\frac{\gamma_z^+}{\beta^+} - \frac{\gamma_z^-}{\beta^-}\right]\rho^+(r) \end{cases}. \tag{A15}$$

We end up with a form of equations that are formally identical to the ones found in the case of a single species with a neutralizing background:

$$\begin{cases} \frac{1}{r}\frac{\partial}{\partial r}\left(\frac{1}{r}\frac{\partial}{\partial r}K(r)\right) = \kappa_\theta e^{-a^+r^2 - b^+G(r) - c^+K(r)} \\ \frac{1}{r}\frac{\partial}{\partial r}\left(r\frac{\partial}{\partial r}G(r)\right) = -\kappa_z e^{-a^+r^2 - b^+G(r) - c^+K(r)} \end{cases}, \tag{A16}$$

where

$$\kappa_{\theta/z} = \frac{\mu_0}{B_0}\left[\frac{\gamma_{\theta/z}^+}{\beta^+} - \frac{\gamma_{\theta/z}^-}{\beta^-}\right]\frac{q^+}{\mathscr{V}^+}, \tag{A17}$$

or with more details

$$\kappa_{\theta/z} = \frac{\mu_0}{B_0}\left[\frac{\gamma_{\theta/z}^+}{\beta^+} - \frac{\gamma_{\theta/z}^-}{\beta^-}\right]\frac{q^+ N^+}{4\pi^2 R \int_0^{+\infty} r e^{-a^+r^2 - b^+G(r) - c^+K(r)} dr}\,. \tag{A18}$$

[1] J. W. Connor, T. Fukuda, X. Garbet, C. Gormezano, V. Mukhovatov, M. Wakatani, and a. ITB Database Group, Nucl. Fusion **44**, R1 (2004).

[2] R. C. Wolf, Plasma Phys. Control. Fusion **45**, R1 (2003).

[3] L. Onsager, Nuovo Cimento, Suppl. **6**, 279 (1949).

[4] S. F. Edwards and J. B. Taylor, Proc. R. Soc. London A **336**, 257 (1974).

[5] J. B. Weiss and J. C. McWilliams, Phys. Fluids A **3**, 835 (1991).

[6] P. H. Chavanis and M. Lemou, Eur. Phys. J. B **59**, 217 (2007).

[7] Y. Elskens and D. F. Escande, *Microscopic Dynamics of Plasmas and Chaos* (IoP Publishing, Bristol, 2002)

[8] D. Bénisti and L. Gremillet, Phys. Rev. E **91**, 042915 (2015).

[9] D. Benisti and L. Gremillet, Phys. Plasmas **14**, 042304 (2007).

[10] R. Bonifacio, Riv. Nuovo Cimento **13**, 1 (1990).

[11] J. Barré, T. Dauxois, G. De Ninno, D. Fanelli, and S. Ruffo, Phys. Rev. E **69**, 045501(R) (2004).

[12] D. Lynden-Bell, Mon. Not. R. Astron. Soc. **136**, 101 (1967).

[13] P. H. Chavanis, G. D. Ninno, D. Fanelli, and S. Ruffo, in *Chaos, Complexity and Transport*, edited by C. Chandre, X. Leoncini, and G. Zaslavsky (World Scientific, Singapore, 2008) pp. 3–26.

[14] M. Antoni and S. Ruffo, Phys. Rev. E **52**, 2361 (1995).

[15] T. Dauxois, S. Ruffo, E. Arimondo, and M. Wilkens, eds., *Dynamics and Thermodynamics of Systems with Long Range Interactions*, Lect. Not. Phys. (Springer-Verlag, Berlin, 2002), Vol. 602.

[16] A. Antoniazzi, D. Fanelli, S. Ruffo, and Y. Y. Yamaguchi, Phys. Rev. Lett. **99**, 040601 (2007).

[17] A. Antoniazzi, D. Fanelli, J. Barre, P.-H. Chavanis, T. Dauxois, and S. Ruffo, Phys. Rev. E **75**, 011112 (2007).

[18] R. Bachelard, C. Chandre, D. Fanelli, X. Leoncini, and S. Ruffo, Phys. Rev. Lett. **101**, 260603 (2008).

[19] X. Leoncini, T. L. Van den Berg, and D. Fanelli, Europhys. Lett. **86**, 20002 (2009).

[20] T. L. Van den Berg, D. Fanelli, and X. Leoncini, Europhys. Lett. **89**, 50010 (2010).

[21] X. Leoncini, in *Nonlinear Dynamics New Directions: Models and Applications*, edited by H. Gonzlez-Aguilar, E. Ugalde, Nonlinear Systems and Complexity (Springer, Cham, 2015), Vol. 12, pp. 79–109.

[22] E. Laribi, S. Ogawa, G. Dif-Pradalier, A. Vasiliev, and X. Leoncini, Fluids **4**, 172 (2019).

[23] S. Ogawa, X. Leoncini, A. Vasiliev, and X. Garbet, Phys. Lett. A **383**, 35 (2019).

[24] W. H. Bennett, Phys. Rev. **45**, 890 (1934).

[25] W. H. Bennett, Phys. Rev. **98**, 1584 (1955).

[26] R. L. Morse, *Equilibria of Collisionless Plasma, Part II*, Tech. Rep. LA-3844(Pt.2), Los Alamos Scientific Lab., N. Mex., 1969.

[27] A. S. Sharma, Nucl. Fusion **23**, 1493 (1983).

[28] A. V. Milovanov and L. M. Zelenyi, Phys. Fluids B **5**, 2609 (1993).

[29] B. Cambon, X. Leoncini, M. Vittot, R. Dumont, and X. Garbet, Chaos **24**, 033101 (2014).

[30] H. Weitzner and D. Pfirsch, Phys. Plasmas **6**, 420 (1999).

[31] J. L. Tennyson, J. R. Cary, and D. F. Escande, Phys. Rev. Lett. **56**, 2117 (1986).

[32] A. I. Neishtadt, Sov. J. Plasma Phys. **12**, 568 (1986).

[33] A. J. Brizard and T. S. Hahm, Rev. Mod. Phys. **79**, 421 (2007).

[34] V. Grandgirard, M. Brunetti, P. Bertrand, N. Besse, X. Garbet, P. Ghendrih, G. Manfredi, Y. Sarazin, O. Sauter, E. Sonnendrücker, J. Vaclavik, and L. Villard, J. Comput. Phys. **217**, 395 (2006).

[35] D. Mihalas and B. Weibel-Mihalas, *Foundations of Radiation Hydrodynamics* (Dover, Mineola, NY, 1999).

[36] A. A. Vlasov, Zh. Eksp. Ther. Fiz. **8**, 291 (1938) [Soviet Physics Uspekhi **10**, 721 (1968)].

[37] C. S. Gardner, Phys. Fluids **6**, 839 (1963).

[38] R. J. J. Mackenbach, J. H. E. Proll, and P. Helander, Phys. Rev. Lett. **128**, 175001 (2022).

[39] W. E. John, B. David, H. Søren, and W. Rik, GNU Octave, version 7.2.0 manual a high-level interactive language for numerical computations, https://docs.octave.org/v7.2.0/.